

Imaging a force field via an optically levitated nanoparticle array

Bihu Lv(吕碧沪), Jiandong Zhang(张建东), and Chuang Li(李闯)

Citation: Chin. Phys. B, 2024, 33 (**9**): 090702. DOI: 10.1088/1674-1056/ad6b86
Journal homepage: http://cpb.iphy.ac.cn; http://iopscience.iop.org/cpb

What follows is a list of articles you may be interested in

Superconducting membrane mechanical oscillator based on vacuum-gap capacitor

Yong-Chao Li(李永超), Xin Dai(戴欣), Jun-Liang Jiang(江俊良), Jia-Zheng Pan(潘佳政), Xing-Yu Wei(魏兴雨), Ya-Peng Lu(卢亚鹏), Sheng Lu(卢盛), Xue-Cou Tu(涂学凑), Guo-Zhu Sun(孙国柱), Pei-Heng Wu(吴培亨)
Chin. Phys. B, 2018, 27 (**6**): 060701. DOI: 10.1088/1674-1056/27/6/060701

Design and characterization of a 3D encapsulation with silicon vias for radio frequency micro-electromechanical system resonator

Ji-Cong Zhao(赵继聪), Quan Yuan(袁泉), Feng-Xiang Wang(王凤祥), Xiao Kan(阚骁), Guo-Wei Han(韩国威), Ling Sun(孙玲), Hai-Yan Sun(孙海燕), Jin-Ling Yang(杨晋玲), Fu-Hua Yang(杨富华)
Chin. Phys. B, 2017, 26 (**6**): 060705. DOI: 10.1088/1674-1056/26/6/060705

Fast filtering algorithm based on vibration systems and neural information exchange and its application to micro motion robot

Gao Wa (高娃), Zha Fu-Sheng (查富生), Song Bao-Yu (宋宝玉), Li Man-Tian (李满天)
Chin. Phys. B, 2014, 23 (**1**): 010701. DOI: 10.1088/1674-1056/23/1/010701

A new magneto-cardiogram study using a vector model with a virtual heart and the boundary element method

Zhang Chen (张琛), Shou Guo-Fa (寿国法), Lu Hong (陆宏), Hua Ning (华宁), Tang Xue-Zheng (唐雪正), Xia Ling (夏灵), Ma Ping (马平), Tang Fa-Kuan (唐发宽)
Chin. Phys. B, 2013, 22 (**9**): 090701. DOI: 10.1088/1674-1056/22/9/090701

Improvement of fabrication and characterization methods for micromechanical disk resonators

Zhao Hui (赵晖), Luo Wei (骆伟), Zheng Hai-Yang (郑海洋), Yang Jin-Ling (杨晋玲), Yang Fu-Hua (杨富华)
Chin. Phys. B, 2012, 21 (**10**): 100702. DOI: 10.1088/1674-1056/21/10/100702

RAPID COMMUNICATION

Imaging a force field via an optically levitated nanoparticle array

Bihu Lv(吕碧沪)[1], Jiandong Zhang(张建东)[2], and Chuang Li(李闯)[1,†]

[1] *Research Center for Novel Computing Sensing and Intelligent Processing, Zhejiang Laboratory, Hangzhou* 311121, *China*
[2] *School of Mathematics and Physics, Jiangsu University of Technology, Changzhou* 213001, *China*

(Received 8 July 2024; revised manuscript received 2 August 2024; accepted manuscript online 6 August 2024)

Levitated optomechanical systems represent an excellent candidate platform for force and acceleration sensing. We propose a force-sensing protocol utilizing an optically levitated nanoparticle array. In our scheme, N nanoparticles are trapped in an optical cavity using holographic optical tweezers. An external laser drives the cavity, exciting N cavity modes interacting simultaneously with the N nanoparticles. The optomechanical interaction encodes the information of the force acting on each nanoparticle onto the intracavity photons, which can be detected directly at the output ports of the cavity. Consequently, our protocol enables real-time imaging of a force field.

Keywords: optomechanics, levitated nanoparticles, force field detection

PACS: 07.10.Cm, 42.50.Lc, 42.50.Wk, 03.67.–a **DOI:** 10.1088/1674-1056/ad6b86

1. Introduction

Optomechanics is a fascinating field that explores the interaction between optical and mechanical degrees of freedom and it has a wide range of applications in various scientific domains.[1–8] Following the pioneering work by Ashkin and Dziedzic,[9–11] levitation of nano- and microscale dielectric objects has become a widely used technique in science[12–14] and engineering.[15–17] An optically levitated dielectric nanoparticle in vacuum serves as an ultrasensitive detector with great potential in precision measurements[18–22] and the study of fundamental physics.[2,23–33] Currently, force sensitivity as low as 10^{-20} N/$\sqrt{\text{Hz}}$[34,35] and sub-$\mu g/\sqrt{\text{Hz}}$ ($g = 9.8$ m/s^2) acceleration sensitivity[36–38] have been demonstrated experimentally. Additionally, as the motion of a levitated dielectric nanoparticle is cooled into the quantum ground state,[39–41] levitated optomechanical systems enter the quantum regime, opening the door to performing interferometry at macroscopic scales to test the limits of quantum superposition principle.[42,43]

Recently, there has been significant interest in the levitation of multiple nanoparticles,[44,45] which holds promise for using arrays of strongly coupled oscillators to explore complex interacting systems and sensing. For example, optically levitated nanoparticles have been used to study the dipole–dipole interaction experimentally[46] and the strong long-range interaction.[47] Theoretical schemes have been proposed to generate the entanglement between the motion of the center of mass of nanoparticles[48,49] by employing an array of optically levitated nanoparticles.

In the field of precision measurement, schemes for gradient measurement using a pair of levitated nanoparticles[50,51] and for acceleration sensing employing an array of levitated nanoparticles[52] have been proposed. However, the measurement of a force field with a three-dimensional space structure utilizing multiple nanoparticles has not yet been explored. Here, we present a force field sensing method using an array of optically levitated nanoparticles, enabling real-time full-profile imaging of a force field.

A simplified schematic of the experimental setup is shown in Fig. 1. Using holographic optical tweezers (HOT),[17,53] N nanoparticles are trapped in a Fabry–Perot cavity. An external laser beam drives the cavity and excites N standing wave cavity modes, which simultaneously interact with the center of mass motion of the N particles. The information of the force impacting each nanoparticle is encoded into the cavity modes through the optomechanical interaction. As a result, detecting the cavity modes with a homodyne detector enables the imaging of the force field.

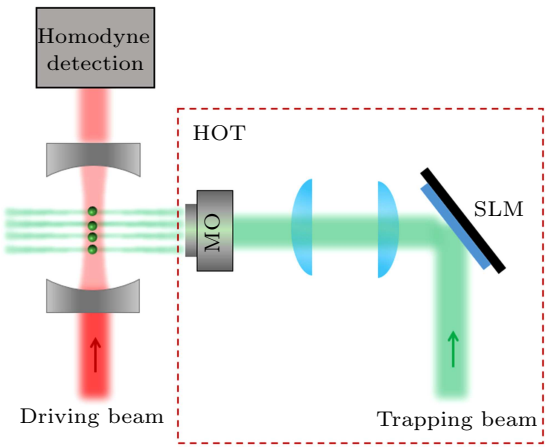


Fig. 1. A simplified schematic of the experimental setup. An array of nanoparticles is trapped in a Fabry–Perot cavity using holographic optical tweezers (HOT). An external laser beam drives the cavity, exciting multiple modes that simultaneously interact with the nanoparticles. The transmission of the cavity mode is monitored by a homodyne detector.

†Corresponding author. E-mail: chuangli_hit@outlook.com

© 2024 Chinese Physical Society and IOP Publishing Ltd

2. Hamiltonian and dynamics

The Hamiltonian of the whole system in a frame rotating at pumping frequency $\nu_{\rm p}^i$ reads

$$\begin{aligned}\frac{\hat{H}}{\hbar} =& \sum_{i=1}^{N}\left[\Delta_{\rm c}^i\hat{a}_i^\dagger\hat{a}_i+\varepsilon_i\left(\hat{a}_i+\hat{a}_i^\dagger\right)\right]+\sum_{i,j=1}^{N}g_{ij}\hat{a}_i^\dagger\hat{a}_i\hat{q}_j\\&+\sum_{j=1}^{N}\left[\frac{\Omega_j}{2}\left(\hat{p}_j^2+\hat{q}_j^2\right)+f_j\hat{q}_j\right],\end{aligned}\tag{1}$$

where $\hat{a}_i$ is the annihilation operator of the ith cavity mode, $\Delta_{\rm c}^i=\omega_{\rm c}^i-\nu_{\rm p}^i$ is the detuning of the ith cavity mode with frequency $\omega_{\rm c}^i$ from the pumping laser, and ε_i is the pump strength. $\hat{q}_j$ and $\hat{p}_j$ denote the dimensionless position and momentum operators of the jth particle, respectively, Ω_j is its oscillation frequency, and f_j is the external force acting on it. g_{ij} is the coupling strength between the ith cavity mode and the jth nanoparticle. This coupling strength depends on the frequency of the cavity mode and the equilibrium position of the nanoparticle (see Appendix A for details).

Under the strong driving condition, each operator can be rewritten as the sum of its classical steady-state mean value and a small quantum fluctuation operator, i.e.,

$$\hat{a}_i\to\alpha_i+\hat{a}_i,\quad \hat{q}_j\to q_j^{\rm s}+\hat{q}_j,\quad \hat{p}_j\to p_j^{\rm s}+\hat{p}_j.\tag{2}$$

Employing the standard linearization procedure,[54] one can obtain the quantum Langevin equations (QLEs) in terms of the quantum fluctuating operators

$$\begin{aligned}\dot{\hat{a}}_i =& -\left(\mathrm{i}\Delta_i+\frac{\kappa_i}{2}\right)\hat{a}_i-\sum_{j=1}^{N}\mathrm{i}G_{ij}\hat{q}_j+\sqrt{\kappa_i}\hat{a}_i^{\rm in},\\ \dot{\hat{q}}_j =& \Omega_j\hat{p}_j,\\ \dot{\hat{p}}_j =& -\Omega_j\hat{q}_j-\gamma_j\hat{p}_j-\sum_{i=1}^{N}G_{ij}\left(\hat{a}_i+\hat{a}_i^\dagger\right)-f_j+\hat{\xi}_j,\end{aligned}\tag{3}$$

where κ_i and γ_j are the decay rates of the ith cavity mode and the jth nanoparticles, respectively. The classical Langevin equations regarding the classical steady-state mean values are presented in Appendix B. $\Delta_i=\Delta_{\rm c}^i+\sum_j g_{ij}q_j^{\rm s}$ and $G_{ij}=\alpha g_{ij}$ are the effective detuning and coupling strength that depend on the steady-state mean values. The operator $\hat{a}_i^{\rm in}$ in Eq. (3) accounts for the input noise of the ith cavity mode, which has zero mean value, and the correlation function

$$\langle\hat{a}_i^{\rm in}(t)\hat{a}_{i'}^{\rm in,\dagger}(t')\rangle=\delta_{ii'}\delta(t-t'),\tag{4}$$

where we have assumed the equilibrium mean photon number of the thermal bath is

$$\bar{n}_i^{\rm c}=\frac{1}{\exp\left[\hbar\omega_{\rm c}^i/k_{\rm B}T\right]-1}\simeq 0$$

due to the high optical frequency $\hbar\omega_{\rm c}^i/k_{\rm B}T\gg 1$, and $\delta_{ii'}$ stands for the Kroneker symbol. $\hat{\xi}_j$ is the input noise of the Brownian force acting on the jth nanoparticle, whose correlation function is given by

$$\begin{aligned}\langle\hat{\xi}_j(t)\hat{\xi}_{j'}(t')\rangle =& \frac{\gamma_j}{\Omega_j}\int\frac{\mathrm{d}\omega}{2\pi}\mathrm{e}^{-\mathrm{i}\omega(t-t')}\omega\\&\times\left[\coth\left(\frac{\hbar\omega}{2k_{\rm B}T}\right)+1\right]\delta_{jj'}.\end{aligned}\tag{5}$$

The involved mechanical frequencies are never larger than hundreds of MHz. Therefore one can make the approximation

$$\frac{\gamma_j}{\Omega_j}\omega\coth\left(\frac{\hbar\omega}{2k_{\rm B}T}\right)\simeq\gamma_j\frac{2k_{\rm B}T}{\hbar\Omega_j}\simeq\gamma_j\left(2\bar{n}_j^{\rm m}+1\right)$$

with the mean thermal phonon number

$$\bar{n}_j^{\rm m}=\left(\exp\left[\hbar\Omega_j/(k_{\rm B}T)\right]-1\right)^{-1}.$$

As a result, the correlation function of Brownian noise can be safely considered Markovian,[54,55] i.e.,

$$\langle\hat{\xi}_j(t)\hat{\xi}_{j'}(t')\rangle\simeq\gamma_j\left(2\bar{n}_j^{\rm m}+1\right)\delta(t-t')\delta_{jj'}.\tag{6}$$

By introducing the amplitude and phase quadrature operators of the cavity field

$$\hat{X}=\frac{\hat{a}+\hat{a}^\dagger}{\sqrt{2}},\quad \hat{Y}=\frac{\hat{a}-\hat{a}^\dagger}{\sqrt{2}\mathrm{i}},\tag{7}$$

the QLEs (3) become

$$\begin{aligned}&\dot{\hat{X}}_i=\Delta_i\hat{Y}_i-\frac{\kappa_i}{2}\hat{X}_i+\sqrt{\kappa_i}\hat{X}_i^{\rm in},\\&\dot{\hat{Y}}_i=-\Delta_i\hat{X}_i-\frac{\kappa_i}{2}\hat{Y}_i-\sqrt{2}\sum_{j=1}^{N}G_{ij}\hat{q}_j+\sqrt{\kappa_i}\hat{Y}_i^{\rm in},\\&\ddot{\hat{q}}_j+\gamma_j\dot{\hat{q}}_j+\Omega_j^2\hat{q}_j=\Omega_j\left(-\sqrt{2}\sum_{i=1}^{N}G_{ij}\hat{X}_i-f_j+\hat{\xi}_j\right).\end{aligned}\tag{8}$$

The QLEs show that the motion of the nanoparticles, $\hat{q}_j$, has a response to the external force field, $\hat{f}_j$. At the same time, the motion information of the nanoparticles is imprinted in the cavity field, $\hat{X}_i$ and $\hat{Y}_i$. As a result, imaging of a force field can be realized through measuring the cavity field.

Transforming the QLEs above into the frequency domain by Fourier transform, one obtains

$$\begin{aligned}\hat{\tilde{X}}_i =& \Delta_i\chi_{\rm c}^i\hat{\tilde{Y}}_i+\sqrt{\kappa_i}\chi_{\rm c}^i\hat{\tilde{X}}_i^{\rm in},\\ \hat{\tilde{Y}}_i =& -\Delta_i\chi_{\rm c}^i\hat{\tilde{X}}_i-\sqrt{2}\chi_{\rm c}^i\sum_{j=1}^{N}G_{ij}\hat{\tilde{q}}_j+\sqrt{\kappa_i}\chi_{\rm c}^i\hat{\tilde{Y}}_i^{\rm in},\\ \hat{\tilde{q}}_j =& \chi_{\rm m}^j\left(-\sqrt{2}\sum_{i=1}^{N}G_{ij}\hat{\tilde{X}}_i-\tilde{f}_j+\hat{\tilde{\xi}}_j\right),\end{aligned}\tag{9}$$

where $\chi_{\rm c}^i=\frac{1}{\kappa_i/2-\mathrm{i}\omega}$ and $\chi_{\rm m}^j=\frac{\Omega_j}{\Omega_j^2-\mathrm{i}\gamma_j\omega-\omega^2}$ are the susceptibilities of the ith cavity mode and the jth nanoparticle, respectively. The susceptibilities describe how an observed quantity responds to a signal or noise.

For the sake of simplicity, we introduce the vector and matrix forms of operators and quantities in QLEs (9), defined as

$$\boldsymbol{X} \equiv \left[\hat{X}_1, \hat{X}_2, \ldots, \hat{X}_N\right]^{\mathrm{T}}, \tag{10}$$

$$\boldsymbol{Y} \equiv \left[\hat{Y}_1, \hat{Y}_2, \ldots, \hat{Y}_N\right]^{\mathrm{T}}, \tag{11}$$

$$\boldsymbol{q} \equiv \left[\hat{q}_1, \hat{q}_2, \ldots, \hat{q}_N\right]^{\mathrm{T}}, \tag{12}$$

$$\boldsymbol{X}^{\mathrm{in}} \equiv \left[\hat{X}_1^{\mathrm{in}}, \hat{X}_2^{\mathrm{in}}, \ldots, \hat{X}_N^{\mathrm{in}}\right]^{\mathrm{T}}, \tag{13}$$

$$\boldsymbol{Y}^{\mathrm{in}} \equiv \left[\hat{Y}_1^{\mathrm{in}}, \hat{Y}_2^{\mathrm{in}}, \ldots, \hat{Y}_N^{\mathrm{in}}\right]^{\mathrm{T}}, \tag{14}$$

$$\boldsymbol{\xi} \equiv \left[\hat{\xi}_1, \hat{\xi}_2, \ldots, \hat{\xi}_N\right]^{\mathrm{T}}, \tag{15}$$

$$\boldsymbol{f} \equiv [f_1, f_2, \ldots, f_N]^{\mathrm{T}}, \tag{16}$$

and

$$\boldsymbol{\Delta} \equiv \begin{bmatrix} \Delta_1 & & \\ & \ddots & \\ & & \Delta_N \end{bmatrix}, \quad \boldsymbol{\kappa} \equiv \begin{bmatrix} \kappa_1 & & \\ & \ddots & \\ & & \kappa_N \end{bmatrix}, \tag{17}$$

$$\boldsymbol{\chi}_{\mathrm{c}} \equiv \begin{bmatrix} \chi_{\mathrm{c}}^1 & & \\ & \ddots & \\ & & \chi_{\mathrm{c}}^N \end{bmatrix}, \quad \boldsymbol{\chi}_{\mathrm{m}} \equiv \begin{bmatrix} \chi_{\mathrm{m}}^1 & & \\ & \ddots & \\ & & \chi_{\mathrm{m}}^N \end{bmatrix}, \tag{18}$$

$$\boldsymbol{G} \equiv \begin{bmatrix} G_{11} & \ldots & G_{1N} \\ \vdots & \ddots & \vdots \\ G_{N1} & \ldots & G_{NN} \end{bmatrix}, \tag{19}$$

where $\boldsymbol{X}$ and $\boldsymbol{Y}$ denote the quadrature operator vector of the cavity field; $\boldsymbol{q}$ denotes the position operator vector of the nanoparticles, $\boldsymbol{X}^{\mathrm{in}}$, $\boldsymbol{Y}^{\mathrm{in}}$, and $\boldsymbol{\xi}$ denote the noise operator vectors of the cavity field and the nanoparticles, respectively; $\boldsymbol{f}$ denotes the force vector of the force field; $\boldsymbol{\Delta}$ and $\boldsymbol{\kappa}$ are the matrices of the detuning and the decay rate of the cavity field, respectively; $\boldsymbol{\chi}_{\mathrm{c}}$ and $\boldsymbol{\chi}_{\mathrm{m}}$ are the matrices of the susceptibilities of the cavity modes and the nanoparticles, respectively; $\boldsymbol{G}$ is the matrix of the coupling strength. The QLEs (9) can be rewritten as

$$\begin{aligned} \boldsymbol{X} &= \boldsymbol{\chi}_{\mathrm{c}}\left(\boldsymbol{\Delta}\boldsymbol{Y} + \sqrt{\boldsymbol{\kappa}}\boldsymbol{X}^{\mathrm{in}}\right), \\ \boldsymbol{Y} &= \boldsymbol{\chi}_{\mathrm{c}}\left(-\boldsymbol{\Delta}\boldsymbol{X} - \sqrt{2}\boldsymbol{G}\boldsymbol{q} + \sqrt{\boldsymbol{\kappa}}\boldsymbol{Y}^{\mathrm{in}}\right), \\ \boldsymbol{q} &= \boldsymbol{\chi}_{\mathrm{m}}\left(-\sqrt{2}\boldsymbol{G}^{\mathrm{T}}\boldsymbol{X} - \boldsymbol{f} + \boldsymbol{\xi}\right). \end{aligned} \tag{20}$$

Solving the above QLEs, the expression of the cavity mode amplitude quadrature operator is given by

$$\begin{aligned} \boldsymbol{X} =\ & \sqrt{2}\boldsymbol{\chi}\boldsymbol{\chi}_{\mathrm{m}}(\boldsymbol{f} - \boldsymbol{\xi}) + \boldsymbol{\chi}\boldsymbol{G}^{-1}\boldsymbol{\chi}_{\mathrm{c}}^{-1}\boldsymbol{\Delta}^{-1}\sqrt{\boldsymbol{\kappa}}\boldsymbol{X}^{\mathrm{in}} \\ & + \boldsymbol{\chi}\boldsymbol{G}^{-1}\sqrt{\boldsymbol{\kappa}}\boldsymbol{Y}^{\mathrm{in}}, \end{aligned} \tag{21}$$

where

$$\boldsymbol{\chi} = \left\{\left[\boldsymbol{G}^{-1}\boldsymbol{\chi}_{\mathrm{c}}^{-1}\boldsymbol{\Delta}^{-1}\boldsymbol{\chi}_{\mathrm{c}}^{-1} + \boldsymbol{G}^{-1}\boldsymbol{\Delta}\right] - 2\boldsymbol{\chi}_{\mathrm{m}}\boldsymbol{G}^{\mathrm{T}}\right\}^{-1}. \tag{22}$$

Using the standard input–output relation $\boldsymbol{X}^{\mathrm{out}} = \boldsymbol{X}^{\mathrm{in}} - \sqrt{\boldsymbol{\kappa}}\boldsymbol{X}$ and the vector of the cavity output field operator

$$\boldsymbol{X}^{\mathrm{out}} \equiv \left[\hat{X}_1^{\mathrm{out}}, \hat{X}_2^{\mathrm{out}}, \ldots, \hat{X}_N^{\mathrm{out}}\right]^{\mathrm{T}}, \tag{23}$$

one obtains

$$\boldsymbol{A}\boldsymbol{X}^{\mathrm{out}} = -\boldsymbol{f} + \boldsymbol{\xi} + \boldsymbol{B}\boldsymbol{X}^{\mathrm{in}} + \boldsymbol{C}\boldsymbol{Y}^{\mathrm{in}} \tag{24}$$

with

$$\boldsymbol{A} = \frac{1}{\sqrt{2}}\boldsymbol{\chi}_{\mathrm{m}}^{-1}\boldsymbol{\chi}^{-1}\sqrt{\boldsymbol{\kappa}^{-1}}, \tag{25}$$

$$\boldsymbol{B} = \boldsymbol{A}\left[\boldsymbol{1} - \sqrt{\boldsymbol{\kappa}}\boldsymbol{\chi}\boldsymbol{G}^{-1}\boldsymbol{\chi}_{\mathrm{c}}^{-1}\boldsymbol{\Delta}^{-1}\sqrt{\boldsymbol{\kappa}}\right], \tag{26}$$

$$\boldsymbol{C} = -\frac{1}{\sqrt{2}}\boldsymbol{\chi}_{\mathrm{m}}^{-1}\boldsymbol{G}^{-1}\sqrt{\boldsymbol{\kappa}}. \tag{27}$$

Equation (24) shows that the information of the force field is encoded in the output field of the cavity via the optomechanical interaction.

According to the definition of the power spectrum density (PSD) for an operator $\hat{O}$ in the frequency domain

$$S_{OO}(\omega) = \int_{-\infty}^{\infty}\langle\hat{O}^{\dagger}(\omega)\hat{O}(\omega')\rangle \mathrm{d}\omega', \tag{28}$$

the PSDs of the force field are given by

$$\begin{aligned} \boldsymbol{S}_{ff}(\omega) =\ & \mathcal{S}_{XX}^{\mathrm{out}}(\omega) - \boldsymbol{S}_{\xi\xi}(\omega) - (\boldsymbol{B}^{*}\circ\boldsymbol{B})\,\boldsymbol{S}_{XX}^{\mathrm{in}}(\omega) \\ & - (\boldsymbol{C}^{*}\circ\boldsymbol{C})\,\boldsymbol{S}_{YY}^{\mathrm{in}}(\omega), \end{aligned} \tag{29}$$

where $\circ$ denotes the Hadamard product and the vectors of PSDs are defined as follows:

$$\boldsymbol{S}_{ff}(\omega) = \left[S_{f_1f_1}(\omega), S_{f_2f_2}(\omega), \ldots, S_{f_Nf_N}(\omega)\right]^{\mathrm{T}}, \tag{30}$$

$$\boldsymbol{S}_{\xi\xi}(\omega) = \left[S_{\xi_1\xi_1}(\omega), S_{\xi_2\xi_2}(\omega), \ldots, S_{\xi_N\xi_N}(\omega)\right]^{\mathrm{T}}, \tag{31}$$

$$\boldsymbol{S}_{XX}^{\mathrm{in}}(\omega) = \left[S_{X_1X_1}^{\mathrm{in}}(\omega), S_{X_2X_2}^{\mathrm{in}}(\omega), \ldots, S_{X_NX_N}^{\mathrm{in}}(\omega)\right]^{\mathrm{T}}, \tag{32}$$

$$\boldsymbol{S}_{YY}^{\mathrm{in}}(\omega) = \left[S_{Y_1Y_1}^{\mathrm{in}}(\omega), S_{Y_2Y_2}^{\mathrm{in}}(\omega), \ldots, S_{Y_NY_N}^{\mathrm{in}}(\omega)\right]^{\mathrm{T}}, \tag{33}$$

$$\mathcal{S}_{XX}^{\mathrm{out}}(\omega) = \left[\mathcal{S}_{XX,1}^{\mathrm{out}}(\omega), \mathcal{S}_{XX,2}^{\mathrm{out}}(\omega), \ldots, \mathcal{S}_{XX,N}^{\mathrm{out}}(\omega)\right]^{\mathrm{T}}. \tag{34}$$

The elements of the vectors $\boldsymbol{S}_{ff}(\omega)$, $\boldsymbol{S}_{\xi\xi}(\omega)$, $\boldsymbol{S}_{XX}^{\mathrm{in}}(\omega)$, and $\boldsymbol{S}_{YY}^{\mathrm{in}}(\omega)$ are calculated through the definition of PSD in Eq. (28). The elements of the vector $\mathcal{S}_{XX}^{\mathrm{out}}(\omega)$ are calculated by

$$\mathcal{S}_{XX,i}^{\mathrm{out}}(\omega) = \sum_{kk'}\boldsymbol{A}_{ik}^{*}(\omega)\boldsymbol{A}_{ik'}(\omega)\boldsymbol{S}_{X_kX_{k'}}^{\mathrm{out}}(\omega) \tag{35}$$

with the definition of the cross-PSD for operators $\hat{P}$ and $\hat{Q}$

$$S_{PQ}(\omega) = \int_{-\infty}^{\infty}\langle\hat{P}^{\dagger}(\omega)\hat{Q}(\omega')\rangle \mathrm{d}\omega'. \tag{36}$$

It is noteworthy that the area under the PSDs of the force yields the variance of the force,[1] i.e.,

$$\langle f_j^2\rangle = \int_{-\infty}^{\infty} S_{f_jf_j}(\omega)\frac{\mathrm{d}\omega}{2\pi}. \tag{37}$$

As shown above, with the measurement results of $\mathcal{S}_{XX}^{\rm out}(\omega)$, the parameters of the system, and Eq. (29), one can obtain the imaging of the force field, the vector $\boldsymbol{S}_{ff}(\omega)$, which contains the information of the force acting on each nanoparticle.

3. Numerical simulation

We numerically simulate the dynamics of a cavity optomechanical system, including N cavity modes and N particles, via the following Markovian master equation:

$$\dot{\hat{\rho}} = \frac{1}{\mathrm{i}\hbar}\left[\hat{\rho}, \hat{H}_{\rm L}\right] + \mathcal{L}(\hat{\rho}), \tag{38}$$

where $\hat{\rho}$ is the density operator of the optomechanical system and

$$\begin{aligned}\frac{\hat{H}_{\rm L}}{\hbar} =& \sum_{i=1}^{N}\Delta_i\hat{a}_i^{\dagger}\hat{a}_i + \sum_{j=1}^{N}\left[\frac{\Omega_j}{2}\left(\hat{p}_j^2+\hat{q}_j^2\right)+f_j(t)\hat{q}_j\right]\\ &+\sum_{i,j=1}^{N}G_{ij}\left(\hat{a}_i^{\dagger}+\hat{a}_i\right)\hat{q}_j\end{aligned} \tag{39}$$

is the linearized Hamiltonian. The Lindblad superoperator $\mathcal{L}(\hat{\rho})$ is given by

$$\begin{aligned}\mathcal{L}(\hat{\rho}) =& \sum_{i=1}^{N}\frac{\kappa_i}{2}\left(2\hat{a}_i\hat{\rho}\hat{a}_i^{\dagger}-\hat{a}_i^{\dagger}\hat{a}_i\hat{\rho}-\hat{\rho}\hat{a}_i^{\dagger}\hat{a}_i\right)\\ &+\sum_{j=1}^{N}\frac{\gamma_j}{2}\left[\bar{n}_j^{\rm m}\left(2\hat{b}_j^{\dagger}\hat{\rho}\hat{b}_j-\hat{b}_j\hat{b}_j^{\dagger}\hat{\rho}-\hat{\rho}\hat{b}_j\hat{b}_j^{\dagger}\right)\right.\\ &\left.+\left(\bar{n}_j^{\rm m}+1\right)\left(2\hat{b}_j\hat{\rho}\hat{b}_j^{\dagger}-\hat{b}_j^{\dagger}\hat{b}_j\hat{\rho}-\hat{\rho}\hat{b}_j^{\dagger}\hat{b}_j\right)\right],\end{aligned} \tag{40}$$

where $\hat{b}_j = (\hat{q}_j + \mathrm{i}\hat{p}_j)/\sqrt{2}$ is the annihilation operator of the jth nanoparticle. Without loss of generality, we assume that the time-dependent external force acting on the jth nanoparticle, $f_j(t)$, is in the form of $f_j(t) = A_{\rm f}^j\cos(\Omega_{\rm f}^j t)$ with the amplitude $A_{\rm f}^j$ and the resonance frequency $\Omega_{\rm f}^j$.

Figure 2 illustrates the numerical results of a cavity optomechanical system containing two cavity modes and two nanoparticles. Figures 2(a), 2(b) and 2(c), 2(d) show the vectors of the PSDs of the cavity output field, $\mathcal{S}_{XX}^{\rm out}(\omega)$, and the external force, $\boldsymbol{S}_{ff}(\omega)$, respectively. The external forces impacting the two nanoparticles are set as $f_1(t) = 0.5\cos(0.3t)$ and $f_2(t) = 0.5\cos(0.5t)$. Two peaks at the frequencies corresponding to that of the external force are observed in both the PSDs of the cavity output field and the force, respectively. The two PSDs of the forces corresponding to the frequencies $\Omega_{\rm f}^1 = 0.3$ and $\Omega_{\rm f}^2 = 0.5$ have an almost equal height (filled area) because of the same amplitude $A_{\rm f}^1 = A_{\rm f}^2 = 0.5$. According to the connection between the variance and the PSD in Eq. (37), we integrate the PSDs around the peaks $\Omega_{\rm f}^1 = 0.3$ and $\Omega_{\rm f}^2 = 0.5$ over the noise floor in (c) and (d) and obtain the variances of the forces $\langle f_1^2\rangle \approx 0.9$ and $\langle f_2^2\rangle \approx 0.8$. These results are consistent with the variances calculated from the analytical expression $\langle f_1^2\rangle = \langle f_2^2\rangle = 0.125$.

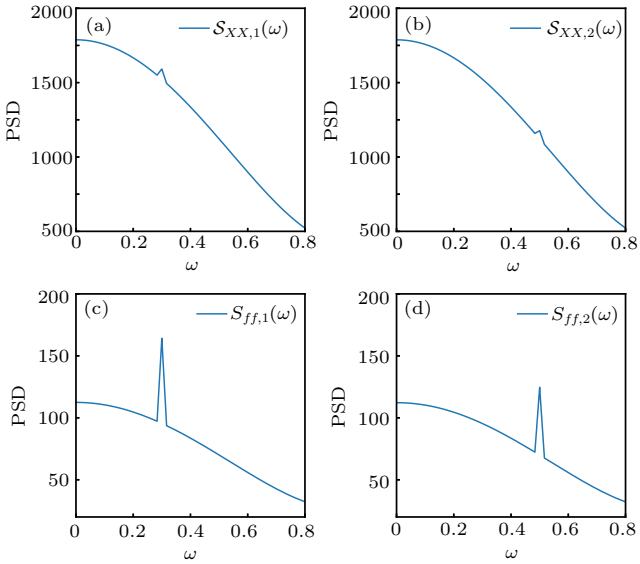


Fig. 2. The results of the numerical simulation: (a), (b) and (c), (d) show the vectors of the PSDs of the cavity output field, $\mathcal{S}_{XX}^{\rm out}(\omega)$, and the external force, $\boldsymbol{S}_{ff}(\omega)$, respectively. The parameters are set as follows: the mechanical frequency $\Omega_1 = \Omega_2 = 1$, the damping rate $\gamma_1 = \gamma_2 = 0.5$, the thermal phonon number $\bar{n}_1^{\rm m} = \bar{n}_2^{\rm m} = 0.1$, the cavity detuning $\Delta_1 = \Delta_2 = 5$, the cavity decay rate $\kappa_1 = \kappa_2 = 10$, the coupling strength $G_{11} = 0.1$, $G_{12} = 0.05$, $G_{21} = 0.05$, and $G_{22} = 0.1$, and the external forces $f_1(t) = 0.5\cos(0.3t)$ and $f_2(t) = 0.5\cos(0.5t)$.

In addition, the numerical results of the external forces with two frequency components, i.e., $f_j(t) = A_{\rm f}^{j1}\cos(\Omega_{\rm f}^{j1}t) + A_{\rm f}^{j2}\cos(\Omega_{\rm f}^{j2}t)$ are also presented in Fig. 3. Similarly, the peaks at the corresponding frequency components of the external force are observed in the PSDs.

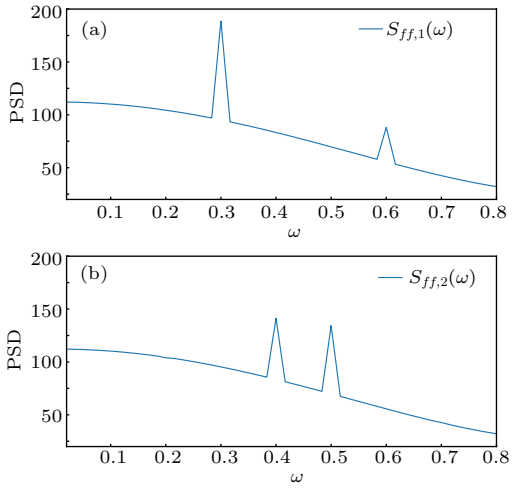


Fig. 3. The results of the numerical simulation: (a) and (b) show the vectors of the PSDs of the external force, $\boldsymbol{S}_{ff}(\omega)$. The external forces are set as follows: $f_1(t) = 0.5\cos(0.3t) + 0.2\cos(0.6t)$ and $f_2(t) = 0.3\cos(0.4t) + 0.4\cos(0.5t)$. The other parameters are the same as those in Fig. 2.

4. Feasibility analysis of the protocol

Our scheme can be realized experimentally by employing holographic optical tweezers trapping multiple nanoparticles

in a driven optical cavity. A feasible experimental realization based on the method in Ref. [46] is given as follows.

As shown in Fig. 1, a trapping beam is expanded to overfill the apertures of the spatial light modulator (SLM) and the microscope objective (MO). The laser beams created by the SLM are imaged with a $4f$ image system onto the MO that creates an array of tightly focused optical tweezers used to trap an array of nanoparticles in a Fabry–Perot cavity. The cavity is driven by another external laser beam (driven beam), allowing multiple excited cavity modes to interact with the nanoparticles.[56–60] The transmission of the cavity modes is monitored through homodyne detection. The coherent scattering and interference effects between the trapping and driven beams are suppressed both by orienting the tweezer polarization along the cavity axis to minimize the mode overlap and by tuning the two lasers far apart in frequency space. By manipulating the phase (and amplitude) of the laser beam using the spatial light modulator, one can precisely trap and move nanoparticles in the cavity. In addition, since the loading of the particle array is probabilistic, a rearrangement protocol utilizing an auxiliary beam[61] can be implemented to improve the success probability of loading.

5. Conclusion and outlook

We have developed a protocol for force field sensing using an array of optically levitated nanoparticles. Employing holographic optical tweezers, N nanoparticles are trapped within a Fabry–Perot cavity. An external laser drives the cavity, exciting N cavity modes interacting simultaneously with the N nanoparticles. The optomechanical interaction encodes the information of the motion of the particles onto the intracavity photons, which can be detected at the cavity output using homodyne detection. Consequently, our protocol enables real-time full-profile imaging and dynamic evolution monitoring of a force field.

In our protocol, multiple cavity modes are used to couple with the motion of the nanoparticles. Although these cavity modes are distinct in the frequency domain, interference between them may occur when a large number of cavity modes are employed. This issue should be studied and addressed in future research. An improved approach may involve using a tunable-frequency cavity mode to replace multiple cavity modes. Furthermore, our protocol currently only images the force field along the cavity axis direction, resulting in one-dimensional imaging of a force field. As a next step, we plan to extend our scheme to achieve three-dimensional imaging of a force field.

Appendix A: The coupling strength between the cavity mode and nanoparticle

In the Rayleigh regime, where the nanoparticle radius is much smaller than the cavity mode wavelength $r \ll \lambda$, a nanoparticle is coupled with the cavity mode through the dipole–dipole interaction, and the interaction Hamiltonian is described by

$$\hat{H}_{ij}^{\mathrm{cav-par}} = -\hbar U_{ij}(\boldsymbol{r})\hat{a}_i^{\dagger}\hat{a}_i, \tag{A1}$$

where we make use of the rotating wave approximation (RWA) and the fast-oscillating terms $\hat{a}_i^{\dagger}\hat{a}_i^{\dagger}$ and $\hat{a}_i\hat{a}_i$ are neglected. The position-dependent cavity frequency shift $U(\boldsymbol{r})_{ij}$ is given by

$$U_{ij}(\boldsymbol{r}) = \frac{3\omega_{\mathrm{c}}^i V_{\mathrm{p}}^j}{2V_{\mathrm{c}}^i}\mathrm{Re}\left(\frac{\varepsilon_{\mathrm{p}}-1}{\varepsilon_{\mathrm{p}}+2}\right)\left|f_{\mathrm{c}}^{ij}(\boldsymbol{r}_j)\right|^2, \tag{A2}$$

where V_{p}^j is the volume of the nanoparticle, V_{c}^i is cavity mode volume, ε_{p} is the electric permittivity of the particle, and

$$\begin{aligned}\left|f_{\mathrm{c}}^{ij}(\boldsymbol{r}_j)\right|^2 &= \left|f_{\mathrm{c}}^{ij}(x_j,y_j,z_j)\right|^2 \\ &= \frac{w_{i,0}^2}{w_i^2(x)}\cos^2(k_i x_j)\exp\left(-\frac{2y_j^2}{w_{i,0}^2}\right)\exp\left(-\frac{2z_j^2}{w_{i,0}^2}\right)\end{aligned} \tag{A3}$$

is the cavity mode profile with the waist $w_{i,0}$ and the wave number $k_i = 2\pi/\lambda_i$ of the cavity mode. Here, the cavity axis is along the x-axis direction. Since the amplitude of the oscillation is small, we can expand the particle motion $\hat{x}$ around the trap position x_j^0 via Taylor expansion and obtain

$$\cos^2(k_i x_j) \approx \cos^2(k_i x_j^0) - \sin(2k_i x_j^0)k_i\hat{x}_j + \mathcal{O}(\hat{x}_j^2). \tag{A4}$$

The linear optomechanical interaction Hamiltonian is given by

$$\hat{H}_{ij}^{\mathrm{linear}} = \hbar g_{ij}\hat{a}_i^{\dagger}\hat{a}_i\hat{x}_j, \tag{A5}$$

where the coupling strength is

$$g_{ij} = \sqrt{2}q_{\mathrm{zp}}^j U_{ij}^0\omega_{\mathrm{c}}^i k_i \sin(2k_i x_j^0)\exp\left(-\frac{2y_j^2}{w_{j,0}^2}\right)\exp\left(-\frac{2z_j^2}{w_{j,0}^2}\right) \tag{A6}$$

with the zero-point fluctuation $q_{\mathrm{zp}}^j = \sqrt{\hbar/(2m_j\Omega_j)}$ and $U_{ij}^0 = \frac{3V_{\mathrm{p}}^j}{2V_{\mathrm{c}}^i}\mathrm{Re}\left(\frac{\varepsilon-1}{\varepsilon+2}\right)$. It shows that the coupling strength g_{ij} is dependent on the frequency ω_{c}^i of the cavity mode and the equilibrium position of the nanoparticle x_j^0.

Appendix B: The classical Langevin equations

Starting from the Hamiltonian (1), by employing the standard linearization procedure,[54] we obtain the quantum Langevin equations QLEs (3) in terms of the quantum fluctuation operators, together with a set of classical Langevin equations (CLEs) in terms of the classical mean values,

$$\dot{\alpha}_i = -\left(\mathrm{i}\Delta_i + \frac{\kappa_i}{2}\right)\alpha_i - \mathrm{i}\varepsilon_i,$$

$$\dot{q}_j^{\rm s} = \Omega_j p_j^{\rm s},$$
$$\dot{p}_j^{\rm s} = -\Omega_j q_j^{\rm s} - \gamma_j p_j^{\rm s} - \sum_{i=1}^{N} g_{ij}|\alpha_i|^2, \tag{B1}$$

where $\Delta_i = \Delta_{\rm c}^i + \sum_j g_{ij} q_j^{\rm s}$. By setting the time derivatives to zero in Eq. (B1), we obtain the steady-state mean values as

$$\alpha_i = \frac{-{\rm i}\varepsilon_i}{{\rm i}\Delta_i + \frac{\kappa_i}{2}}, \quad p_j^{\rm s} = 0, \quad q_j^{\rm s} = -\sum_{i=1}^{N} \frac{g_j|\alpha_i|^2}{\Omega_j}, \tag{B2}$$

which determine the effective detuning and coupling strength in QLEs (3) in the main text.

Acknowledgements

We thank Tongtong Zhu for the useful discussion. This work is supported by the Natural Science Foundation of Zhejiang Province (Grant No. LQ22A040010) and the National Natural Science Foundation of China (Grant Nos. 12304545 and 12204434).

References

[1] Aspelmeyer M, Kippenberg T J and Marquardt F 2014 *Rev. Mod. Phys.* **86** 1391
[2] Nie W, Lan Y, Li Y and Zhu S 2014 *Sci. China Phys. Mech. Astron.* **57** 2276
[3] Liu Y C, Hu Y W, Wong C W and Xiao Y F 2013 *Chin. Phys. B* **22** 114213
[4] Mahajan S, Aggarwal N, Bhattacherjee A B, *et al.* 2013 *Chin. Phys. B* **23** 020315
[5] Liu Y l, Wang C, Zhang J and Liu Y X 2018 *Chin. Phys. B* **27** 024204
[6] Wang Y P, Zhang Z C, Yu Y F and Zhang Z M 2019 *Chin. Phys. B* **28** 014202
[7] Zhang S, Li T, Duan Q H, Zhang J Q and Bao W S 2021 *Chin. Phys. B* **30** 023701
[8] Liu Y Y, Zhang Z M, Liu J H, Wang J D and Yu Y F 2022 *Chin. Phys. B* **31** 094203
[9] Ashkin A and Dziedzic J 1971 *Appl. Phys. Lett.* **19** 283
[10] Ashkin A and Dziedzic J 1976 *Appl. Phys. Lett.* **28** 333
[11] Ashkin A and Dziedzic J 1977 *Appl. Phys. Lett.* **30** 202
[12] Ashkin A, Dziedzic J M and Yamane T 1987 *Nature* **330** 769
[13] Ashkin A and Dziedzic J M 1987 *Science* **235** 1517
[14] Fazal F M and Block S M 2011 *Nat. Photon.* **5** 318
[15] Dholakia K and Čižmár T 2011 *Nat. Photon.* **5** 335
[16] Padgett M and Bowman R 2011 *Nat. Photon.* **5** 343
[17] Maragò O M, Jones P H, Gucciardi P G, Volpe G and Ferrari A C 2013 *Nat. Nanotechnol.* **8** 807
[18] Ranjit G, Atherton D P, Stutz J H, Cunningham M and Geraci A A 2015 *Phys. Rev. A* **91** 051805
[19] Ranjit G, Cunningham M, Casey K and Geraci A A 2016 *Phys. Rev. A* **93** 053801
[20] Hempston D, Vovrosh J, Toroš M, Winstone G, Rashid M and Ulbricht H 2017 *Appl. Phys. Lett.* **111** 133111
[21] Hebestreit E, Frimmer M, Reimann R and Novotny L 2018 *Phys. Rev. Lett.* **121** 063602
[22] Blakemore C P, Rider A D, Roy S, Wang Q, Kawasaki A and Gratta G 2019 *Phys. Rev. A* **99** 023816
[23] Li T, Kheifets S, Medellin D and Raizen M G 2010 *Science* **328** 1673
[24] Li T and Raizen M G 2013 *Annalen der Physik* **525** 281
[25] Gieseler J, Novotny L and Quidant R 2013 *Nat. Phys.* **9** 806
[26] Gieseler J, Quidant R, Dellago C and Novotny L 2014 *Nat. Nanotechnol.* **9** 358
[27] Jain V, Gieseler J, Moritz C, Dellago C, Quidant R and Novotny L 2016 *Phys. Rev. Lett.* **116** 243601
[28] Rondin L, Gieseler J, Ricci F, Quidant R, Dellago C and Novotny L 2017 *Nat. Nanotechnol.* **12** 1130
[29] Arvanitaki A and Geraci A A 2013 *Phys. Rev. Lett.* **110** 071105
[30] Monteiro F, Afek G, Carney D, Krnjaic G, Wang J and Moore D C 2020 *Phys. Rev. Lett.* **125** 181102
[31] Moore D C, Rider A D and Gratta G 2014 *Phys. Rev. Lett.* **113** 251801
[32] Rider A D, Moore D C, Blakemore C P, Louis M, Lu M and Gratta G 2016 *Phys. Rev. Lett.* **117** 101101
[33] Carney D, Krnjaic G, Moore D C, Regal C A, Afek G, Bhave S, Brubaker B, Corbitt T, Cripe J, Crisosto N, *et al.* 2021 *Quantum Science and Technology* **6** 024002
[34] Tebbenjohanns F, Frimmer M, Militaru A, Jain V and Novotny L 2019 *Phys. Rev. Lett.* **122** 223601
[35] Tebbenjohanns F, Frimmer M, Jain V, Windey D and Novotny L 2020 *Phys. Rev. Lett.* **124** 013603
[36] Monteiro F, Ghosh S, Fine A G and Moore D C 2017 *Phys. Rev. A* **96** 063841
[37] Rider A D, Blakemore C P, Gratta G and Moore D C 2018 *Phys. Rev. A* **97** 013842
[38] Monteiro F, Li W, Afek G, Li C l, Mossman M and Moore D C 2020 *Phys. Rev. A* **101** 053835
[39] Delić U, Reisenbauer M, Dare K, Grass D, Vuletić V, Kiesel N and Aspelmeyer M 2020 *Science* **367** 892
[40] Magrini L, Rosenzweig P, Bach C, Deutschmann-Olek A, Hofer S G, Hong S, Kiesel N, Kugi A and Aspelmeyer M 2021 *Nature* **595** 373
[41] Tebbenjohanns F, Mattana M L, Rossi M, Frimmer M and Novotny L 2021 *Nature* **595** 378
[42] Romero-Isart O, Juan M L, Quidant R and Cirac J I 2010 *New J. Phys.* **12** 033015
[43] Romero-Isart O, Pflanzer A C, Blaser F, Kaltenbaek R, Kiesel N, Aspelmeyer M and Cirac J I 2011 *Phys. Rev. Lett.* **107** 020405
[44] Hüpfl J, Bachelard N, Kaczvinszki M, Horodynski M, Kühmayer M and Rotter S 2023 *Phys. Rev. Lett.* **130** 083203
[45] Hüpfl J, Bachelard N, Kaczvinszki M, Horodynski M, Kühmayer M and Rotter S 2023 *Phys. Rev. A* **107** 023112
[46] Rieser J, Ciampini M A, Rudolph H, Kiesel N, Hornberger K, Stickler B A, Aspelmeyer M and Delić U 2022 *Science* **377** 987
[47] Vijayan J, Piotrowski J, Gonzalez-Ballestero C, Weber K, Romero-Isart O and Novotny L 2024 *Nat. Phys.* **20** 859
[48] Rudolph H, Hornberger K and Stickler B A 2020 *Phys. Rev. A* **101** 011804
[49] Brandão I, Tandeitnik D and Guerreiro T 2021 *Quantum Science and Technology* **6** 045013
[50] Li C, Li Y, Hu H and Dong Y 2022 *Sci. China Phys. Mech. Astron.* **65** 240311
[51] Rudolph H, Delić U, Aspelmeyer M, Hornberger K and Stickler B A 2022 *Phys. Rev. Lett.* **129** 193602
[52] Li Y, Li C, Zhang J, Dong Y and Hu H 2023 *Phys. Rev. Appl.* **20** 024018
[53] Gieseler J, Gomez-Solano J R, Magazzù A, Castillo I P, García L P, Gironella-Torrent M, Viader-Godoy X, Ritort F, Pesce G, Arzola A V, *et al.* 2021 *Advances in Optics and Photonics* **13** 74
[54] Genes C, Vitali D, Tombesi P, Gigan S and Aspelmeyer M 2008 *Phys. Rev. A* **77** 033804
[55] Genes C, Vitali D and Tombesi P 2008 *New J. Phys.* **10** 095009
[56] Gopalakrishnan S, Lev B L and Goldbart P M 2009 *Nat. Phys.* **5** 845
[57] Wickenbrock A, Hemmerling M, Robb G R M, Emary C and Renzoni F 2013 *Phys. Rev. A* **87** 043817
[58] Kollár A J, Papageorge A T, Vaidya V D, Guo Y, Keeling J and Lev B L 2017 *Nat. Commun.* **8** 14386
[59] Vaidya V D, Guo Y, Kroeze R M, Ballantine K E, Kollár A J, Keeling J and Lev B L 2018 *Phys. Rev. X* **8** 011002
[60] Guo Y, Kroeze R M, Vaidya V D, Keeling J and Lev B L 2019 *Phys. Rev. Lett.* **122** 193601
[61] Yan J, Yu X, Han Z V, Li T and Zhang J 2023 *Photonics Research* **11** 600